

Article

Not peer-reviewed version

Influence of Key Strata on the Evolution Law of Mining-induced Stress in the Working Face of Deep and Large-scale Mining

[Jianlin Xie](#) , [Shan Ning](#) ^{*} , [Weibing Zhu](#) , [Xiaozhen Wang](#) , Tao Hou

Posted Date: 23 June 2023

doi: 10.20944/preprints202306.1691.v1

Keywords: key strata; mining-induced stress; DOFS; 3DEC; large-scale mining



Preprints.org is a free multidiscipline platform providing preprint service that is dedicated to making early versions of research outputs permanently available and citable. Preprints posted at Preprints.org appear in Web of Science, Crossref, Google Scholar, Scilit, Europe PMC.

Copyright: This is an open access article distributed under the Creative Commons Attribution License which permits unrestricted use, distribution, and reproduction in any medium, provided the original work is properly cited.

Article

Influence of key strata on the evolution law of mining-induced stress in the working face of deep and large-scale mining

Jianlin Xie ¹ and Shan Ning ^{2,*}, Weibing Zhu ², Xiaozhen Wang ², Tao Hou ³

¹ State Key Laboratory of Coal Exploration and Intelligent Mining, China University of Mining and Technology, Xuzhou, Jiangsu 221116, China; xjlin@cumt.edu.cn (J.X.)

² School of Mines, China University of Mining and Technology, Xuzhou, Jiangsu 221116, China; ning-shan@cumt.edu.cn (S.N.); zweibing@163.com (W.Z.); cumtwxz@cumt.edu.cn (X.W.);

³ Shaanxi Zhengtong Coal Industry Co. LTD, Xianyang, Shaanxi 713600, China; houtao202204@163.com (T.H.)

* Correspondence: ningshan@cumt.edu.cn (S.N.)

Abstract: When there are multiple key strata in the overburden of deep coal seam and the surface subsidence coefficient after mining is small, it indicates that the overlying key strata fail to break completely after mining. On this occasion, the stress concentration on the working face occurs easily, which in turn leads to the occurrence of dynamic disasters such as rock burst. This study adopted a comprehensive analysis method of field monitoring and numerical simulation to explore the influence of key stratum on the evolution law of mining-induced stress in the working face. Distributed optical fiber sensor (DOFS) and surface subsidence GNSS monitoring system were respectively arranged inside and at the mouth of the ground observation borehole. According to the monitoring results of strain obtained from DOFS, the height of broken stratum inside the overlying strata was obtained; according to the monitoring results of surface subsidence, the surface subsidence coefficient was proved to be less than 0.1, indicating that the high key stratum does not break completely, but enters a state of bending subsidence instead. In order to reveal the influence of key stratum on the mining-induced stress of working face, two 3DEC numerical models with and without key stratum were established for comparative analysis. As the numerical simulation results show, when there are multiple key strata in the overburden, the stress influence range and stress concentration coefficient of coal seam after mining are relatively large. The study revealed the working mechanism of rock burst accidents after large-scale mining and predicted the potential area of rock burst risk after the mining of the working face, which has been verified by field investigation. The research results are of great guiding significance for the revelation of the working mechanism of rock burst in deep mining condition and its prevention and control.

Keywords: key strata; mining-induced stress; DOFS; 3DEC; large-scale mining

1. Introduction

The movement of overlying strata after coal mining will exert some impact on the stress evolution of underground working face. The key stratum plays a major role in bearing the overlying strata [1]. Accordingly, it is of particular importance to master the influence of the key stratum distribution in the overlying strata on the evolution of mining-induced stress in the working face.

Mining-induced stress distribution of the working face in a kilometer-deep coal mine has been studied [2]. Different key stratum thicknesses and heights have been numerically simulated by the Universal Distinct Element Code (UDEC) software in order to study the effect of key stratum on the mining abutment pressure of a coal seam [3]. The distribution of energy accumulation and fracture positions before and after the fracture of overlying key strata are derived, and the energy release of

fractures in each stratum is calculated [4]. The mechanism and evolution control of pillar bursts in multithick key strata are studied using field investigation, theoretical analysis, and numerical simulation [5]. The spatial fracture characteristic of overlying strata was analyzed by Winkler elastic foundation beam theory [6]. Based on the Key strata theory an overburden caving model is proposed to predict the multilayered hard strata behaviour [7]. A new damage model based on the modified thermomechanical continuum constitutive model in coal mass and the contact layers between the rock and coal mass is proposed [8]. Fracture failure analysis of hard and thick key layer and its dynamic response characteristics were analyzed [9]. Strata movement and stress evolution when mining two overlapping panels affected by hard stratum has been studied [10]. The analysis of the distribution characteristics of the primary key stratum in the coal mine reveals the bow-shaped structural characteristics of the overlying thick primary key stratum [11]. The mechanism, prevention measures, and control methods for earthquake disasters typically occurring in mines with thick and hard rock strata were investigated [12]. A simplified mechanical model for the analysis of dynamic destabilization of the overlying strata during underground mining was constructed [13]. A study investigated the spatiotemporal effect of mining-induced stress-fracture-seepage field coupling, characterized by ladder key stratum and composite aquifer [14]. Wilson's equations for the vertical stress distribution in the vicinity of a single longwall panel after it has been mined have been used in conjunction with finite element modelling to evaluate vertical stresses in the underlying strata [15]. An estimation method for cover pressure re-establishment distance and pressure distribution in the goaf of longwall coal mines [16]. Gravitational rules are used as the basis for the prognosis of vertical stress distribution in exploited rock masses [17]. To analyze the law of movement and caving of the roof rock stratum, the roof subsidence displacement, rock stratum stress, and the rock stratum movement law were analyzed by using the methods of the particle discrete element and similar material simulation test [18]. Based on the analysis of subsidence and overlying structural characteristics, the influencing factors and the control effect laws of strata movement were investigated [19].

A working face in Binchang mining area of China is buried nearly a kilometer deep, with a mining height of over 10m. After coal mining, the surface subsidence is generally slight, and the underground rock burst accidents occur frequently, indicating that the movement law of the overlying strata is of certain particularity. Through field monitoring and numerical simulation, this study explored the strata movement law of the mine after mining and analyzed the influence of the key stratum of overlying strata on the evolution of mining-induced stress in the working face, laying the foundation for revealing the mechanism of rock burst.

2. Project overview

The plane layout of the working face in the mine under study is shown in Figure 1. First, the four working faces LW101~ LW104 in panel 1 were mined; then LW201~ LW 205 in panel 2 were mine successively; then LW302 in panel 3 were mined; and LW 301 in panel 3 was mined finally. This study mainly analyzed the evolution law of mining-induced stress after mining LW204 and LW205, and then LW302 and LW301.

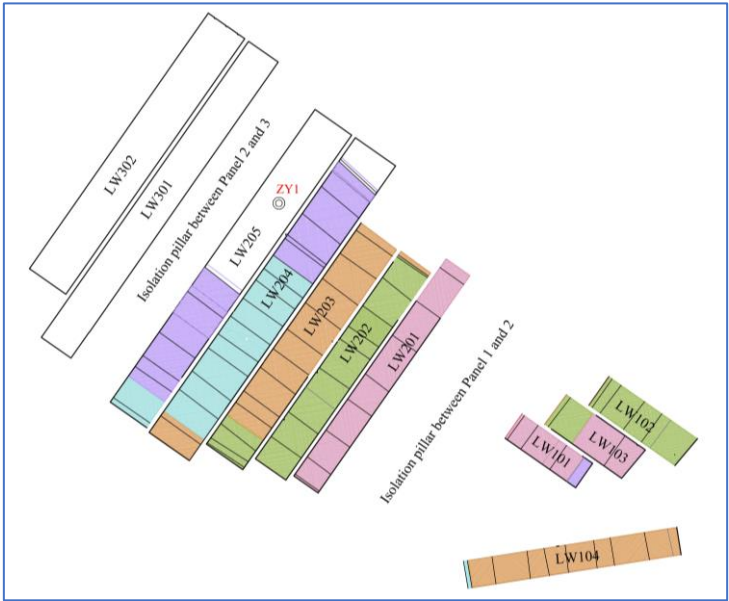


Figure 1. The layout of working faces in the panels.

3. Field monitoring

In order to master the internal movement law of overlying strata, an observation borehole ZY1 was arranged on the ground surface of LW205 with a depth of 940m (the layout position is shown in Figure 1). A dual-channel DOFS with a depth of 930m was arranged inside the borehole (the scheme is shown in Figure 2(a)), and the on-site installation process is shown in Figure 2(b). Meanwhile, a set of GNSS system was also arranged on the surface to monitor the changes in surface subsidence in real time (Figure 2(c)).

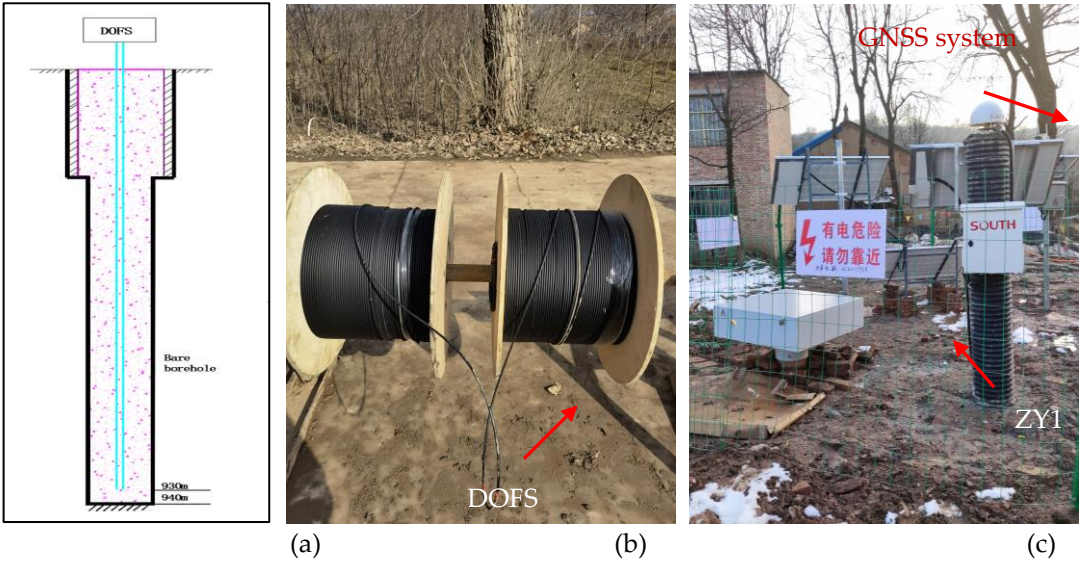


Figure 2. The on-site installation and equipment of observation borehole ZY1: (a) Observation scheme; (b) On-site installation; (c) Monitoring equipment.

After the drilling of observation borehole ZY1 was completed, the corresponding columnar distribution results of strata were obtained by logging in the hole. By means of the key stratum discrimination software, the ZY1 column was judged and the key stratum distribution was obtained, as shown in Figure 3. It can be seen from Figure 3 there are 14 key strata in the whole overburden above the coal seam.

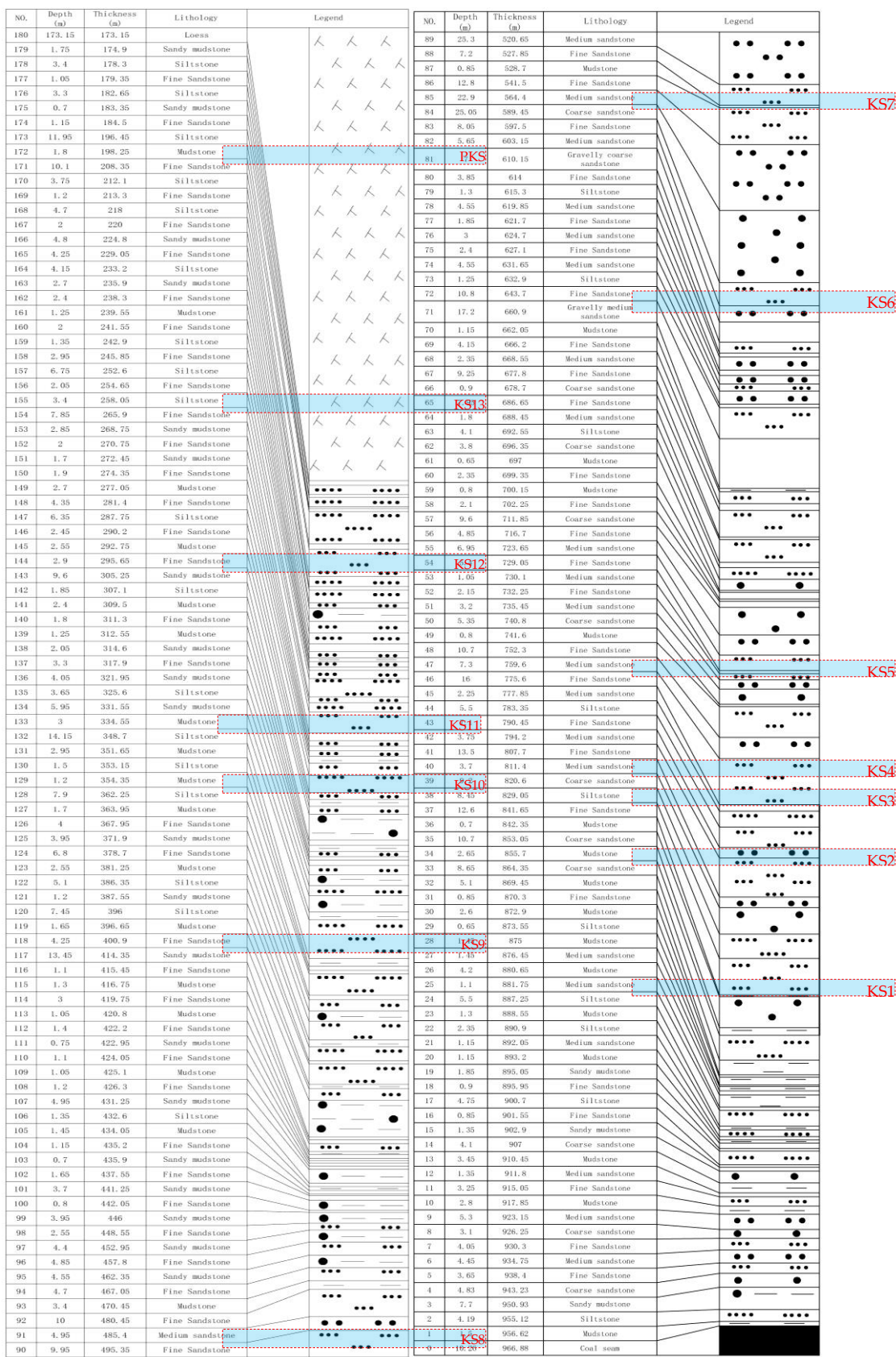


Figure 3. ZY1column and discrimination results of key strata.

With ZY1 being 292m ahead of the working face, the installation of DOFS in the borehole and GNSS monitoring system for surface subsidence was completed on November 27, 2020 and strain measuring was conducted for the first time. From then on, strain measuring was conducted regularly

until October 26, 2021 when the mining in the working face was over. At that time, the working face had advanced beyond ZY1 by 380.4m. Even after the mining in the working face was over, strain measuring was still conducted for many times; and the last measuring was conducted on December 6, 2021. The strain value measured at the first time was set as the benchmark; then the strain data obtained from each subsequent measuring was conducted overall differential processing with the benchmark. The strain difference curves obtained are shown in Figure 4. As can be seen, the negative value in the vertical coordinate represents that the rock formation is under compressive strain, while the positive value indicates that the rock formation is under tensile strain.

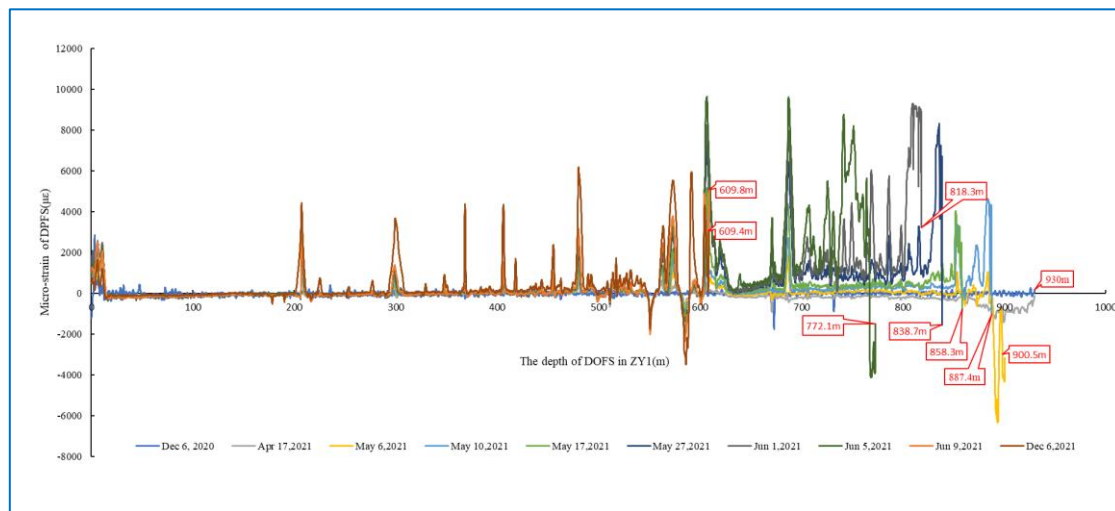


Figure 4. The in-situ strain curves of DOFS during the mining pocess of LW205.

As can be seen from Figure 4, when ZY1 was ahead of the working face (the corresponding mining time was before May 10, 2021), the overlying strata were affected by the advance stress. On May 6, 2021, when ZY1 was 12.6m ahead of the working face, the DOFS at a depth of 900.5m in the borehole was broken because the compression was beyond its strain limit.

On May 10, 2021, when the working face advanced past ZY1 by 0.5m, the strain form of the DOFS in the borehole changed from compressive strain to tensile strain and the DOFS broke at the depth of 887.4m, which corresponded to KS1 in the borehole.

On May 17, 2021, when the working face advanced past ZY1 by 18.4m, the DOFS broke at the depth of 853.7m, which corresponded to KS2 in the borehole.

On May 27, 2021, when the working face advanced past ZY1 by 47.6m, the DOFS broke at the depth of 838.7m, which corresponded to KS3 in the borehole.

On June 1, 2021, when the working face advanced past ZY1 by 61.3m, the DOFS broke at the depth of 818.3m, which corresponded to KS4 in the borehole.

On June 5, 2021, when the working face advanced past ZY1 by 71.3m, the DOFS broke at the depth of 772.1m, which corresponded to KS5 in the borehole.

On June 9, 2021, when the working face advanced past ZY1 by 81.5m, the DOFS broke at the depth of 609.8m, which corresponded to the range between KS6 and KS7 in the borehole. Since then, as the working face continued to advance, the breakpoint height of the DOFS tended to be stable.

On October 26, 2021, when the mining on the working face was over, the working face had advanced past ZY1 by 380.4m. On December 6, 2021, the strain was measured for the last time, which revealed that the stain value increased slightly but the position of breakpoint remained unchanged. This indicates that the high overlying strata above KS7 remained a basically stable state.

In addition to the above regular monitoring of DOFS in the borehole, real-time monitoring of the surface subsidence near the mouth of ZY1 was conducted and the corresponding curve was obtained, as shown in Figure 5. As can be seen, when the working face advanced past ZY1 by 380m, the corresponding surface subsidence data is approximately 588mm. Since the mining height of LW205

is 10m, the corresponding subsidence ratio is about 0.058, indicating that the overlying strata is not broken yet and in a state of bending deformation.

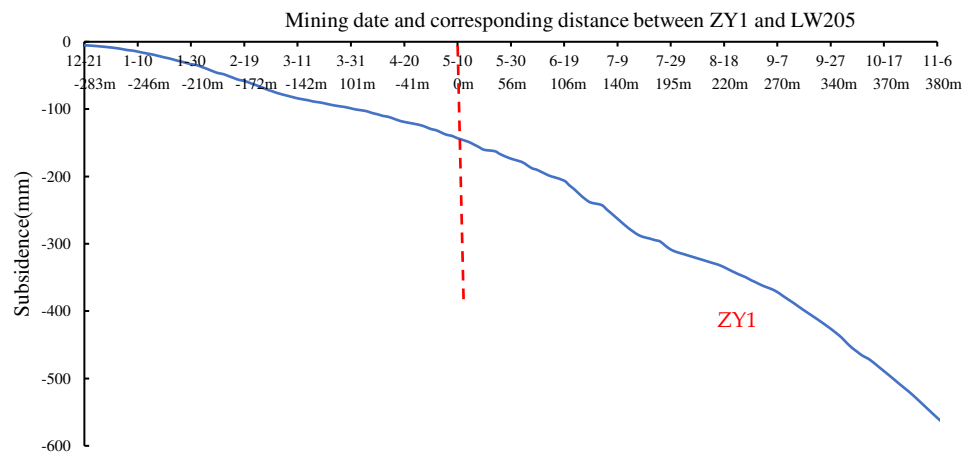


Figure 5. The in-situ surface subsidence curve of ZY1 after LW205 mining.

4. Numerical simulation

4.1. Simulation schemes

Based on the columnar distribution of rock strata in the three panels and actual geological data, the numerical model was established by using 3DEC discrete element software. By using discrete element method, the rock mass is treated as blocks which can produce displacement and torsion motion. In this way, 3DEC discrete element software can effectively simulate the phenomena of fracture, separation, deformation and failure of surrounding rock. According to the key stratum theory, the key stratum controls the deformation and fracture of the whole overlying rock. Therefore, the key stratum in Figure 3 is retained in the model, while other rock strata are replaced by homogenized soft rock. In order to facilitate the simulation, the strike dimensions of the working face in tpanel 2 and panel 3 in Figure 1 are uniformly processed, and the plane layout of the working face in the model is shown in Figure 6.

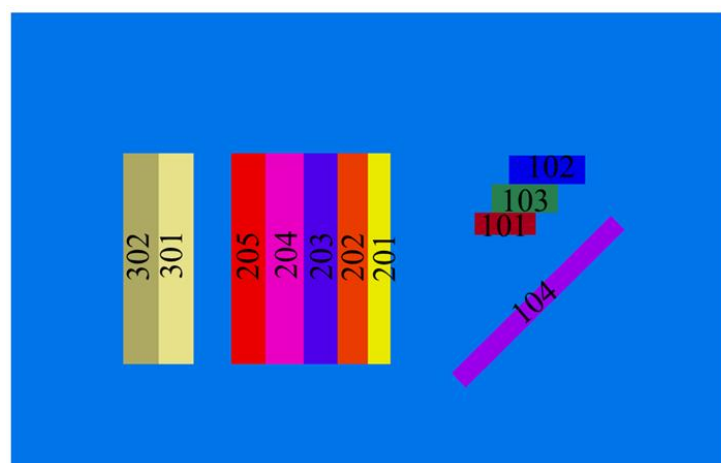


Figure 6. The working faces plan of discrete element model.

A 3D numerical model (4100m×2600m×500m) was established (as shown in Figure 7(a)) to simulate the mining process of three panels and analyze the evolution law of mining-induced stress in the coal seam. In the mining process, one working face is excavated each time, and the excavation

sequence is as follows: panel 1, panel 2, LW302, and LW301. After the excavation is over, the model will be calculated to reach a state of equilibrium again. In order to conduct a comparative analysis of the influence law of key stratum on the evolution of mining-induced stress, the block and joint strength of key stratum is weakened on the basis of the model in Figure 7(a), and a weakened model without key stratum is obtained, as shown in Figure 7(b).

Since the purpose of this study is to obtain the stress evolution law of the surrounding rock and the failure law of roof strata in the mining process, the thickness of floor in the model is slightly smaller. At the same time, in order to eliminate the boundary effect, a distance of more than 600m is reserved on both sides of the working face. Given that the burial depth of the working face is nearly one kilometer, in order to facilitate the model calculation, the top boundary of the model is constrained by uniform load on the premise that the simulation results are not to be affected. To be specific, a vertical stress of 13.2 MPa is applied in accordance with the burial depth of the model. Meanwhile, the horizontal and vertical constraints are applied to the surrounding boundary and the bottom boundary respectively, and their displacement is fixed to 0. Based on the geological histogram of the area under study, the numerical model is built layer by layer from the bottom boundary according to the actual thickness and lithology of the rock (coal) layer. This model design is more complex in structure, but it can simulate the movement of the roof of the coal seam more realistically and accurately.

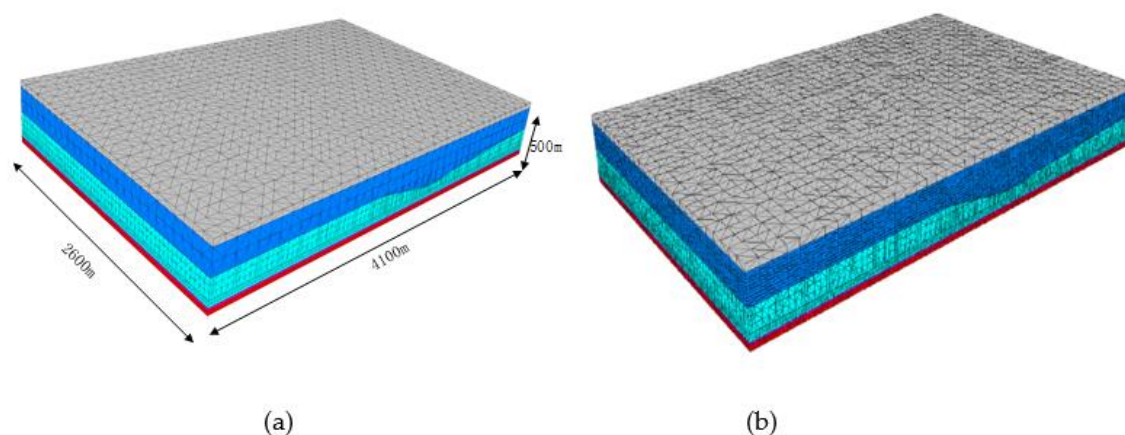


Figure 7. The stereogram of three-dimensional discrete element model: (a) The actual model; (b) The weakened model.

In order to make the simulation results more aligned with the actual situation, the inversion modeling is carried out based on the field measured surface subsidence data. The simulated surface subsidence curve of LW205 after mining in Model 7(a) is shown in Figure 8. When the working face is pushed 380m past the observation point, the surface subsidence is 590mm, which is basically consistent with the measured results in Figure 5, indicating that the actual model established is in line with the actual mining conditions, thus ensuring the reliability of subsequent simulation results.

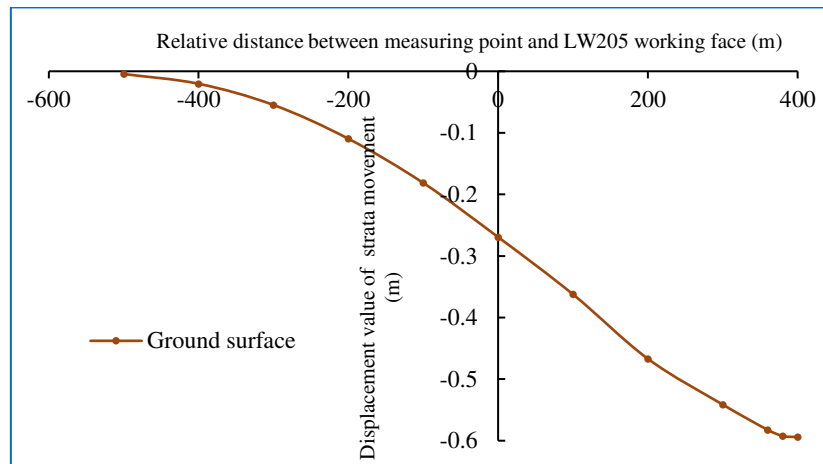


Figure 8. The simulated surface subsidence curve after LW205 mining in actual model.

4.2. The evolution law of mining-induced stress in panel 1 and panel 2

With the progress of working face, the equilibrium state of rock mass around the stope is broken, and the gravity of overlying rock strata in the goaf is transferred to the surrounding coal body. Within a certain range around the stope, the vertical stress of the coal seam increases significantly, forming stress concentration. In the actual mining process, when the working faces of LW201~LW204 were mined, many rock burst accidents occurred in the main roadway in the isolated coal pillar area between panel 1 and panel 2.

In order to analyze the stress distribution of the surrounding rock of the stope in the mining process, the vertical stress distribution cloud map (Figure 9) of the coal seam was derived for analysis after the mining of LW204.

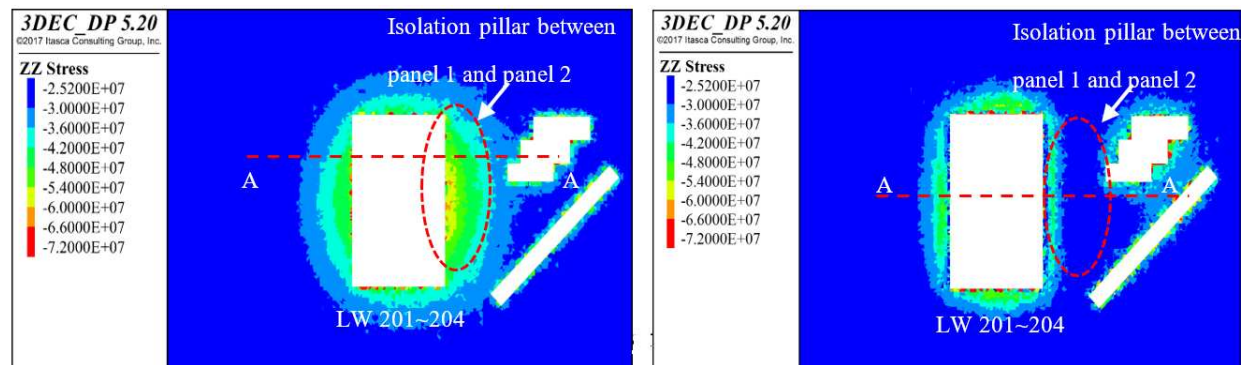


Figure 9. The cloud map of vertical stress distribution in the coal seam after the mining of LW204:

(a)The actual model;(b)The weakened model.

(As is shown in Figure 9(a), the bearing stress around the goaf increases to a large extent after the working face in the first panel and LW201~204 working faces are mined. Comparative speaking, the stress increases mildly around the goaf in the first panel, whereas the stress increases significantly in the second panel. Figure 9(b) shows that the stress increase in the coal pillar area between the first panel and the second panel is not noticeable after the key stratum is weakened.

In order to further explain the distribution law of mining-induced stress in the first and second panels, measuring line A-A was set in the first panel and the second panel to monitor the vertical stress data. The vertical stress curve of LW204 after mining working face was obtained, as shown in Figure 10.

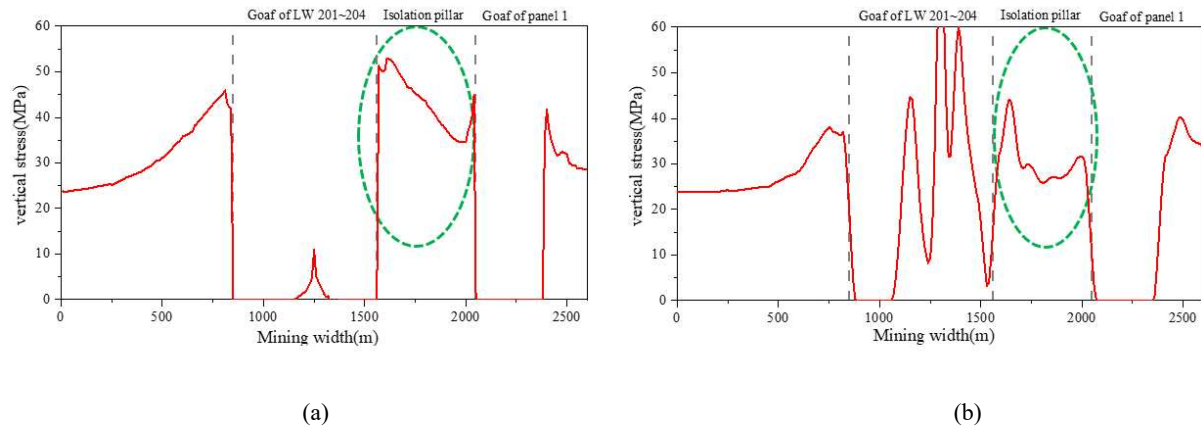


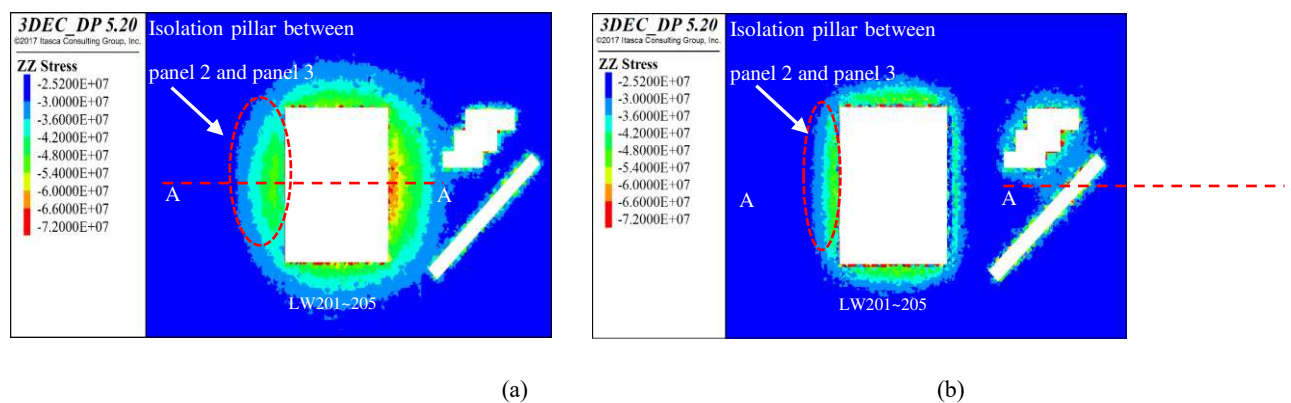
Figure 10. The vertical stress curve in the coal seam after the mining of LW204: (a)The actual model; (b)The weakened model.

As is shown in Figure 10(a), when panel 1 and LW201~204 in panel 2 are mined, the vertical stress in the isolated coal pillar area between panel 1 and panel 2 appears trapezoidal distribution with one side high and the other side low; and the stress at the edge of the goaf in panel 2 is obviously higher than that at the edge of panel 1. In the isolated coal pillar area between panel 1 and panel 2, the stress increases significantly. The average stress is about 43MPa, and the stress concentration coefficient reaches 1.79. When the key stratum is weakened, the stress increase in the isolated coal pillar area between panel 1 and panel 2 is not obvious (as shown in Figure 10(b)), the average stress in this area is about 32Mpa, and the stress concentration coefficient reaches 1.33.

The above simulation results show that the key stratum existing in the overlying strata has a significant influence on the mining-induced stress evolution of the coal seam. Moreover, the results also reveal the mechanism of rock burst accidents in the main roadway in the isolated coal pillar area between panel 1 and panel 2 after the mining of LW201-204 working faces.

4.3. The evolution law of mining-induced stress in panel 2 and panel 3

With the increase of goaf area, the stress of coal seam around the goaf further increases. Especially when panel 2 is mined, the goaf is virtually one kilometer wide and the whole panel is basically in a full-mining state. As the mining continues in panel 3, the stress in the isolated coal pillar area between panel 2 and panel 3 witnesses a significant change. Therefore, the vertical stress distribution cloud map and stress curve of coal seam are derived for further analysis after LW205 and LW302 are mined. Figure 11 and 12 show the cloud map and stress curve corresponding to the two working faces respectively.



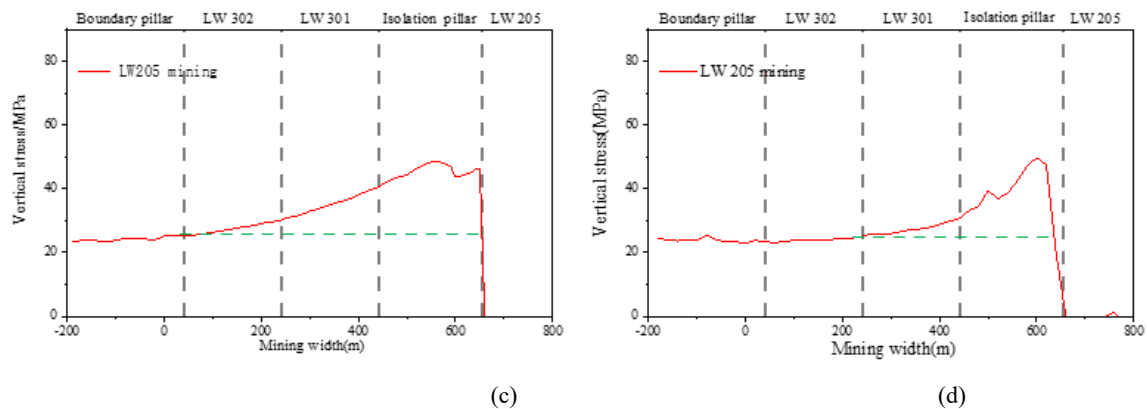


Figure 11. The vertical stress distribution cloud map and stress curve in the coal seam after the mining of LW205: (a)The cloud map of actual model;(b)The cloud map of weakened model; (c)The stress curve of actual model;(d)The stress curve of weakened model.

Theoretically, the stress influence boundary should be divided according to the standard that the bearing stress should be more than 1.05 time of the original stress. As can be seen from Figure 11, when LW205 in panel 2 is mined, the influence range of the lateral bearing stress is 660m. However, the influence range of lateral bearing stress in the weakened model is reduced to 400m.

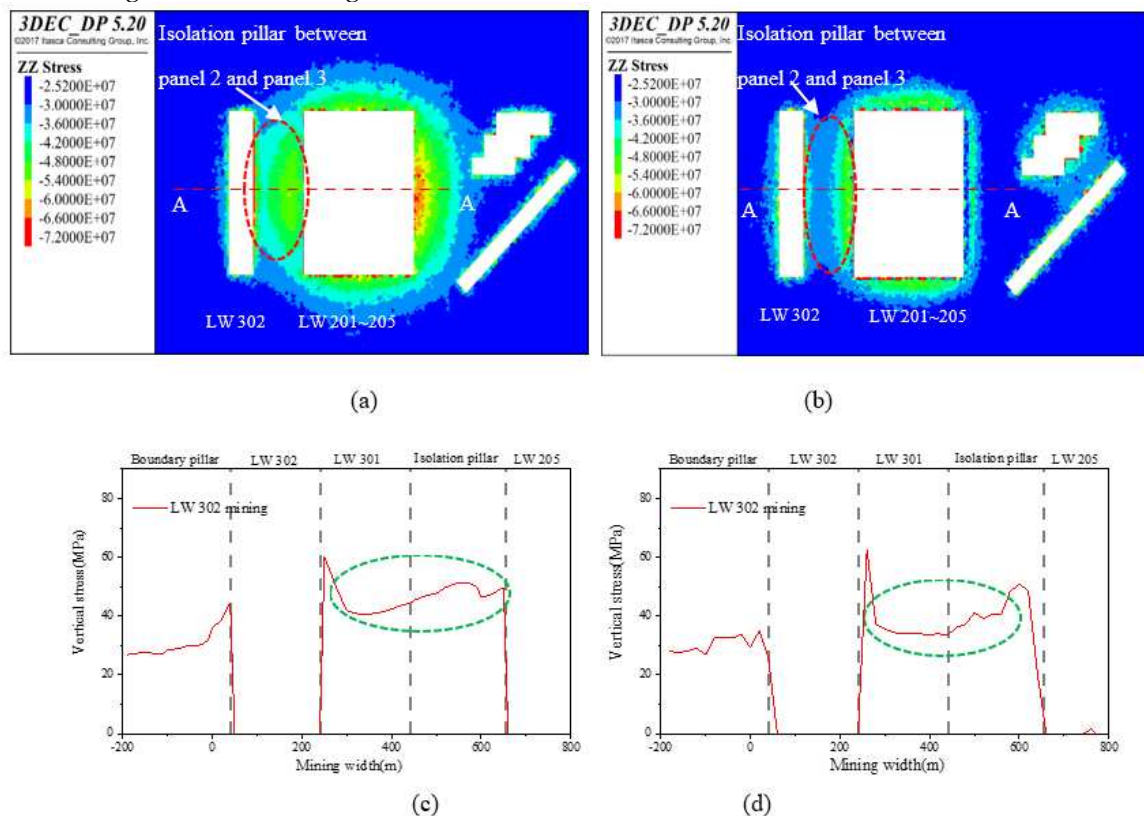


Figure 12. The vertical stress distribution cloud map and stress curve in the coal seam after the mining of LW302: (a)The cloud map of actual model;(b)The cloud map of weakened model; (c)The stress curve of actual model;(d)The stress curve of weakened model.

As can be seen from Figure 12, due to the mining of panel 3, the vertical stress in the isolated coal pillar area between panel 2 and panel 3 rises and a high stress zone is formed noticeably. As LW302 is mined, stress concentration occurs in the isolated coal pillar area between panel 2 and panel 3. The stress in the area is generally over 40 MPa, with the peak value reaching 60.24 MPa and the

stress concentration coefficient being as high as 2.51. This indicates that when LW302 is mined, its adjacent working face LW301 is in a state of high stress. In other words, the risk of rock burst is rather high in the mining process. However, in the weakened model, no obvious stress concentration occurs in LW301 and the stress in the central part of isolated coal pillar area between panel 2 and panel 3 does not increase significantly.

With the mining of LW301, the stress in the isolated coal pillar area between panel 2 and panel 3 would display a further rising trend. After LW301 reaches a state of equilibrium, the vertical stress distribution cloud map and stress curve of coal seam are derived, as shown in Figure 13.

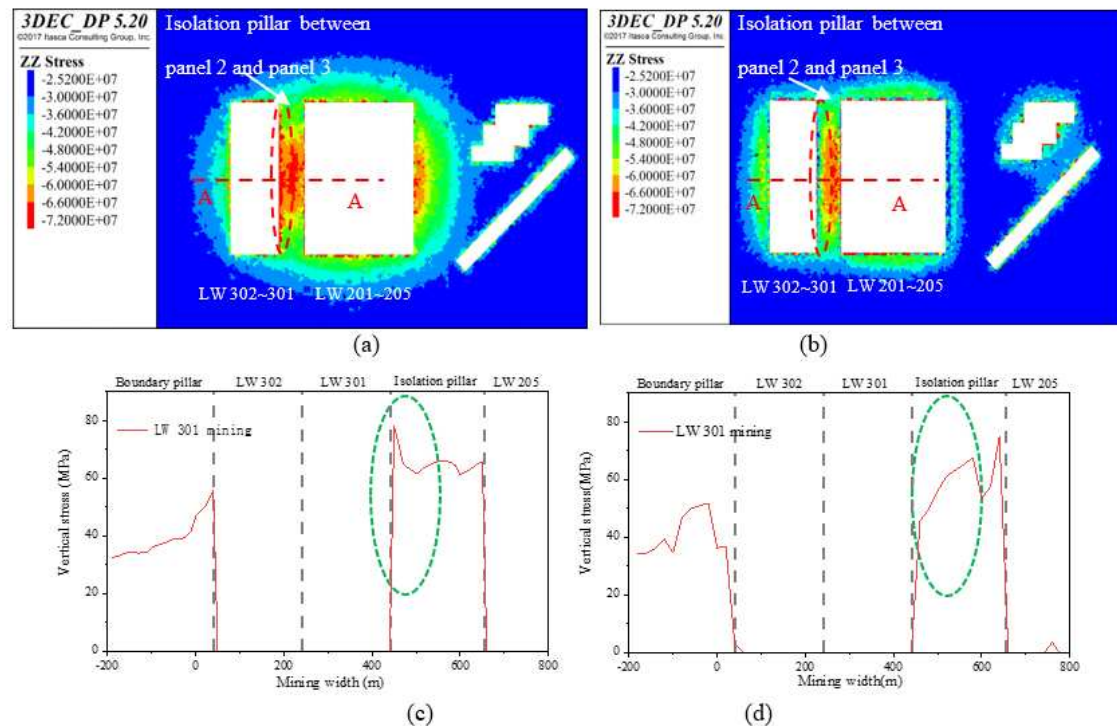


Figure 13. The vertical stress distribution cloud map and stress curve in the coal seam after the mining of LW301: (a)The cloud map of actual model; (b)The cloud map of weakened model; (c)The stress curve of actual model; (d)The stress curve of weakened model.

As is shown in Figure 13(a), due to the mining of LW301, the stress in the isolated coal pillar area between panel 2 and panel 3 displays a relatively remarkable rising trend. The maximum stress in the central part of isolated coal pillar area between panel 2 and panel 3 reaches up to 72 MPa, with the stress concentration coefficient being as high as 2.92. This peak value is far higher than the vertical stress in other areas around the goaf in panel 3. As can be seen from Figure 13(b), when the key stratum is weakened, no obvious high stress zone is observed near the coal pillar side in LW301.

Figure 13(c) shows that the stress in the coal pillar area increases further after LW301 is mined. The average vertical stress upon the isolated coal pillars between panel 2 and panel 3 increases by 17MPa. In particular, the stress of LW301 return airway near the coal pillar side increases by about 30MPa compared to LW302 after mining. As can be known from Figure 13(d), when the key stratum is weakened, stress concentration is not obvious in LW301 return airway. This indicates that due to the influence of the key stratum of overlying strata, the rock burst risk of the return airway along the coal pillar side is greater in the mining process of LW301. Accordingly, the anti-shock and pressure relief measures should be taken in advance to ensure the safety during the mining period. As is revealed through field investigation, during the mining process of LW301, several roof-fall events occurred in the return airway, which verifies the correctness of the simulation results.

5. Conclusions

(1) The ground observation borehole was arranged in the test mine; and DOFS and the surface subsidence GNSS monitoring system were installed inside and at the mouth of the borehole respectively. According to the monitoring data on strain obtained by DOFS, the height of the broken stratum in the overlying rock after mining is much lower than that of the main key stratum, indicating that through fracture does not occur in the high key strata. As the monitoring results of the GNSS monitoring system show, the surface subsidence volume is 0.058m, and the subsidence coefficient is less than 0.1. This verifies again that the high key strata don't break and enters a state of bending subsidence instead.

(2) By comparing the simulation results, it is found that when there are multiple key strata in the overlying strata, the stress concentration on the isolated coal pillar between panel 1 and panel 2 is greatly affected after the mining of LW201-LW204. This reveals the working mechanism of rock burst accidents in the main roadway in the isolated coal pillar area between panel 1 and panel 2.

(3) By comparing the simulation results, it is predicted that when there are multiple key strata in the overlying strata, the stress concentration risk of LW301 return airway along the coal pillar between panel 2 and panel 3 is relatively higher compared to LW302 after mining. After the actual mining, several roof-fall events occurred in the return airway, which verifies the accuracy of the predicted results.

(4) The paper reveals the mechanism of rock burst accidents caused by the significant influence of multiple key strata in the overlying strata on stress concentration in coal seam. Moreover, it predicts the potential hazard areas after mining. The research results are of great guiding significance for the prevention and control of rock burst accidents.

Author Contributions: Conceptualization, J.X. and W.Z.; formal analysis, J.X. and S.N.; writing—original draft preparation, J.X. and S.N.; writing—review and editing, W.Z. and X.W.; investigation, J.X. and T.H.; validation, W.Z. and X.W.; All authors have read and agreed to the published version of the manuscript.

Funding: National Natural Science Foundation of China (52274097). The project is also funded by Shaanxi Zhengtong Coal Industry Co. Ltd., Shandong Energy, China.

Institutional Review Board Statement: Not applicable.

Informed Consent Statement: Not applicable.

Data Availability Statement: The data presented in this study are available on request from the corresponding author.

Acknowledgments: We extended our sincere thanks to the relevant staff at the State Key Laboratory of Coal Exploration and Intelligent Mining for the simulation experiment.

Conflicts of Interest: The authors declare no conflict of interest.

References

1. Qian, M.G.; Miao, X.X.; Xu, J.L. Theoretical study of key stratum in ground control. *J. Chin. Coal Soc.* **1996**, *21*, 225-230.
2. Xie, J.L.; Xu, J.L.; Wang, F. Mining-induced stress distribution of the working face in a kilometer deep coal mine - a case study in Tangshan coal mine. *J. Geophys. Eng.* **2018**, *15*, 2060-2070.
3. Xie, J.L.; Xu, J.L. Effect of key stratum on the mining abutment pressure of a coal seam. *Geosci. J.* **2017**, *21*, 267-276.
4. Liu, H.; Yu, B.; Liu, J.R.; Wang, T.X. Investigation of impact rock burst induced by energy released from hard rock fractures. *Arab. J. Geosci.* **2019**, *12*, 381.
5. Guo, W.H.; Cao, A.Y.; Xue, C.C.; Hu, Y.; Wang, S.W.; Zhao, Q. Mechanism and evolution control of wide coal pillar bursts in multithick key strata. *Shock Vib.* **2021**, *2021*, 4696619.
6. Yang, Z.Q.; Liu, C.; Zhu, H.Z.; Xie, F.X.; Dou, L.M.; Chen, J.H. Mechanism of rock burst caused by fracture of key strata during irregular working face mining and its prevention methods. *Int. J. Rock Mech. Min.* **2019**, *29*, 889-897.
7. Zhu, Z.J.; Wu, Y.L.; Han, J.; Chen, E. Overburden failure and ground pressure behaviour of longwall top coal caving in hard multi-layered roof. *Arch. Min. Sci.* **2019**, *64*, 575-590.

8. Tahmasebinia, F.; Zhang, C.G.; Canbulat, I.; Sepasgozar, S.; Saydam, S. A novel damage model for strata layers and coal mass. *Energies*, **2020**, *13*, 1928.
9. Jiang, L.S.; Wu, Q.S.; Wu, Q.L.; Wang, P.; Xue, Y.C.; Kong, P.; Gong, B. Fracture failure analysis of hard and thick key layer and its dynamic response characteristics. *Eng. Fail. Ana.*, **2019**, *98*, 118-130.
10. Zhang, J.G.; Yang, W.; Lin, B.Q.; Zhang, J.J.; Wang, M. Strata movement and stress evolution when mining two overlapping panels affected by hard stratum. *Int. J. Rock Mech. Min.* **2019**, *29*, 691-699.
11. Ning, S.; Zhu, W.B.; Xie, J.L.; Song, S.K.; Wang, X.Z.; Yu, D.; Lou, J.F.; Xu, J.L. Influence of stress distribution in coal seams of non-uniform extremely thick key stratum and disaster-causing mechanisms. *Sci. Rep-UK*, **2022**, *12*, 14465.
12. Zhang, M.; Hu, X.L.; Huang, H.T.; Chen, G.Y.; Gao, S.; Liu, C.; Tian, L.H. Mechanism and prevention and control of mine earthquake in thick and hard rock strata considering the horizontal stress evolution of stope. *Shock Vib.* **2021**, *2021*, 6680928.
13. Lv, X.F.; Zhou, H.Y.; Wang, A.W.; Feng, C.; Xiao, X.C. Characteristics of stress transfer and progressive fracture in overlying strata due to mining-induced disturbances. *Adv Civ. Eng.* **2018**, *2018*, 8967010.
14. Zhang, T.; Gan, Q.; Zhao, Y.X.; Zhu, G.P.; Nie, X.D.; Yang, K.; Li, J.Z. Investigations into mining-induced stress-fracture-seepage field coupling effect considering the response of key stratum and composite aquifer. *Rock Mech. Rock Eng.* **2019**, *52*, 4017-4031.
15. Suchowerska, A.M.; Merifield, R.S.; Carter, J.P. Vertical stress changes in multi-seam mining under supercritical longwall panels. *Int. J. Rock Mech. Min.* **2013**, *61*, 306-320.
16. Yavuz, H. An estimation method for cover pressure re-establishment distance and pressure distribution in the goaf of longwall coal mines. *Int. J. Rock Mech. Min.* **2004**, *41*, 193-205.
17. Jirankova, E.; Petros, V.; Sancer, J. The assessment of stress in an exploited rock mass based on the disturbance of the rigid overlying strata. *Int. J. Rock Mech. Min.* **2012**, *50*, 77-82.
18. Liu, W.R. Experimental and numerical study of rock stratum movement characteristics in longwall mining. *Shock Vib.* **2019**, *2019*, 5041536.
19. Zhang, G.J.; Wang, Z.Y.; Guo, G.L.; Wei, W.; Wang, F.G.; Zhong, L.L.; Gong, Y.Q. Study on regional strata movement during deep mining of Erdos coal field and its control. *Int. J. Env. Res. Pub. He.* **2022**, *19*, 14902.